Applied Catalysis B: Environmental 152–153 (2014) 38–45

Contents lists available at ScienceDirect

Applied Catalysis B: Environmental

journal homepage: www.elsevier.com/locate/apcatb

Review

Gold in CO oxidation and PROX: The role of reaction exothermicity and nanometer-scale particle size

Mikhail Kipnis*

A.V. Topchiev Institute of Petrochemical Synthesis RAS, 29 Leninsky Prospect, 119991 Moscow, Russia

ARTICLE INFO

Article history:
Received 21 October 2013
Received in revised form 10 January 2014
Accepted 15 January 2014
Available online 22 January 2014

Keywords:
CO oxidation
Preferential CO oxidation
Gold
Surface ignition
Size distribution

ABSTRACT

Gold is a promising catalyst for various processes. There have been extensive studies in catalysis using Au-containing catalysts, but their results are ambiguous, prompting researchers to revise the data available from the literature.

In this work, we analyze publications on CO oxidation and PROX (preferential CO oxidation) over various supported gold catalysts, focusing on two important aspects: effect of high exothermicity of the reaction and of nanometer-scale particle of gold. Under certain conditions, exothermicity brings the reaction into the external diffusion control regime, causing the so-called ignition of the catalyst surface. The transition of the reaction to this regime is accompanied by a number of effects (sharp increase in conversion as a result of increasing temperature, CO conversion hysteresis, appearance of a hot spot in the catalyst bed, change in activation energy, and precursor self-activation), which are misinterpreted by researchers sometimes. The behavior of the catalyst in the steady-state external diffusion control regime and on return from this regime is discussed.

In the synthesis of gold catalysts by conventional methods (precipitation, deposition–precipitation, impregnation), the precursors dried at 100 °C have gold mostly in its cationic form. The gold cations turn into Au^0 as the calcination temperature is raised or as the catalyst is kept in a reductive atmosphere. This yields gold metal particles on the support surface. Their size distribution is usually asymmetric, with the maximum shifted to smaller sizes, which is typical of lognormal distribution.

A critical review is made of the data concerning the size effect, specifically, the existence of an extremum of catalytic activity as a function of the mean particle size. It is demonstrated that the variation of gold content from one sample to another is often disregarded in the interpretation of these data, while catalytic activity and particle size correlate with gold content.

Contents

1. Introduction 39
2. External diffusion control regime of a very exothermic reaction 39
   2.1. Transition of the reaction to the external diffusion control regime 39
   2.2. Temperature and feed flow rate effects in the operation in the external diffusion control regime: Hysteresis 40
   2.3. Factors hampering the transition of the reaction to the CSI regime 41
3. Behavior of nanosized gold 42
   3.1. Particle size distribution of gold metal 42
   3.2. On the "size effect" in gold catalysts 42
4. Conclusions 44
   Acknowledgments 44
   References 44

* Tel.: +7 495 954 13 95; fax: +7 495 633 85 20.
E-mail address: kipnis@ips.ac.ru

0926-3373/$ – see front matter © 2014 Elsevier B.V. All rights reserved.
http://dx.doi.org/10.1016/j.apcatb.2014.01.030

1. Introduction

There is keen interest in the use of gold in various catalytic reactions, which has been stimulated by studies of gold-catalyzed CO oxidation carried out by Haruta and his colleagues [1–4]. It was discovered that gold shows good catalytic properties in CO oxidation even well below the room temperature. There have been extensive studies on the applicability of Au-containing catalysts to other reactions [4–8].

Although publications on CO oxidation alone run into hundreds, gold-containing catalysts and the reactions in which they are involved are still complicated objects for the researcher.

Various aspects of the synthesis of supported catalysts have been examined [9–21]; the role of certain factors in CO oxidation has also been elucidated. It was established that water exerts a favorable effect on CO oxidation [9,22–35]; for this, a reaction mechanism involving a hydroperoxide as an intermediate was suggested [36]. The activity of the catalyst in CO oxidation was enhanced by hydrogen [37–43]; the mechanism of CO oxidation in the presence of H_2 [37] is also based on the formation of hydroperoxide as an intermediate.

The state of active gold, the causes of catalyst deactivation, the irreproducibility of catalytic tests in some cases, the catalyst aging, and the effect of support still remain unresolved issues.

The authors of a review [44] distinguish four significant yet not fully comprehensible features of Au-catalyzed CO oxidation: the process is support-dependent; gold must be in oxidized state to display a high catalytic activity; the activity of the catalyst is sensitive to the presence of water in the feedstock; the activity of Au nanoparticles is very high and depends strongly on their size and morphology.

Containing comparatively smaller amounts of gold in the form of finely dispersed particles, the gold catalysts are difficult to characterize by physicochemical methods. The parameters of their X-ray photoelectron spectra (peak position and half-width) depend on the Au cluster size: as the cluster size decreases, the peak broadens and shifts to higher binding energies [45]. The X-ray photoelectron spectrum of oxidized gold nanoparticles changes under the action of X-rays [46]. Additional problems arise from the fact that the catalysts change their properties on prolonged storage [14,47–50].

Although some authors hypothesize that cationic gold is essential for CO oxidation [51–61], it is obvious that it occurs on gold metal. For this reason, many publications on CO oxidation present transmission electron microscopic data characterizing the gold metal particles. The presence of gold as metal particles suggests that, when the gas medium contains reducing agents such as H_2 and CO, cationic gold turns into Au^0 provided that the treatment time is sufficient for its reduction.

The CO oxidation reaction (as well as H_2 oxidation) is highly exothermic. Accordingly, the amount of heat released in the reaction zone increases with the amount of converted carbon monoxide (H_2), and the reaction may shift from kinetic control to external diffusion control (e.g. [42,62–65] and references therein).

Using the Pt, Ru, Rh, Au catalyst series as an example, we have demonstrated the specific features of the reaction transition to the external diffusion control regime as well as those of the steady state in this regime [42,62,66–71]. These features are not always considered in the investigation of CO oxidation and PROX (preferential CO oxidation). This prompted us to examine them in detail in the context of relevant publications.

The following aspects were left out of consideration in this work: the mechanism of oxygen activation on gold, the mechanisms of CO and PROX, the role of cationic gold, the contribution from the support to catalysis, effects of H_2O and CO_2 on catalysis.

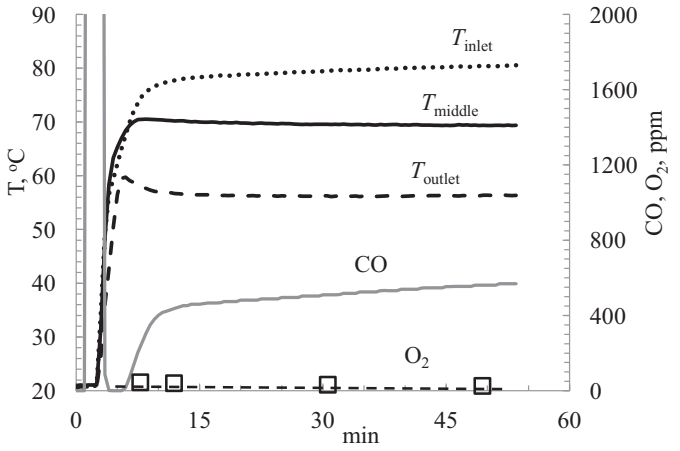

Fig. 1. Preferential oxidation of CO over 1% Au/Al_2O_3 catalyst (a bed height of ~1.6 cm) by the gas mixture (composition, vol%: O_2—0.9, CO—0.9, H_2—60, N_2—balance) at room temperature. Transition into the steady-state CSI. The temperature at the bed: inlet—T_{inlet}, outlet—T_{outlet}, and the middle of the bed—T_{middle}. GHSV 41 N l/g_{cat}/h.

2. External diffusion control regime of a very exothermic reaction

Strongly exothermic reactions typically take place in the external diffusion control regime, in which the activity of the catalyst is determined by the rate at which the critical component is supplied and, accordingly, depends on the reaction temperature only weakly. Frank-Kamenetskii [72] termed the transition of a reaction to this regime and the steady-state run of the reaction in this regime as catalyst surface ignition (CSI).

The reactions proceeding in the CSI regime include industrial ammonia oxidation [73]; ethylene hydrogenation over a Pt/boehmite catalyst [74]; selective acetylene and ethylene hydrogenation over Pd/Al_2O_3 [75]; *para*-methylstyrene, octene, and heptene hydrogenation over a Pd- or Pt-containing catalyst [76]; total CO and CH_4 oxidation over Pt/Al_2O_3 and Pt/CeO_2 catalysts [64]; CO oxidation [63–65,74,75,77,78]; partial CH_4 oxidation [79]; and propane oxidation [80].

Researchers usually focus on the effect of temperature on the behavior of the reactants, whereas temperature distribution in the catalyst bed is also of significance [42,62,66–71,77,79,81,82].

Below, we will discuss some features of the transition of a reaction to the CSI regime using selective CO oxidation and PROX as the examples.

2.1. Transition of the reaction to the external diffusion control regime

It was reported [71] that the reaction shifts readily from 1%Au/Al_2O_3 catalyst preactivated in a mixture containing CO, O_2, and H_2 to external diffusion control regime after replacing H_2 with the reaction mixture at room temperature. This transition is illustrated in Fig. 1, which shows the dynamics of the bed temperature and residual CO and O_2 concentrations.

The reaction mixture was initially by-passed (1.5 min), then switched over (2.5 min) to the reactor filled with H_2. The appearance of the reaction mixture in the reactor caused a rapid heating of the catalyst bed. This was indicated by thermocouples placed at the bed inlet (T_{inlet}), in the middle of the bed (T_{middle}), and at the bed outlet (T_{outlet}). However, in a few minutes the temperature at the reactor outlet decreased after passing through a maximum and a temperature gradient across the bed was established with a hot spot located at the bed inlet, which is typical of CSI. When the

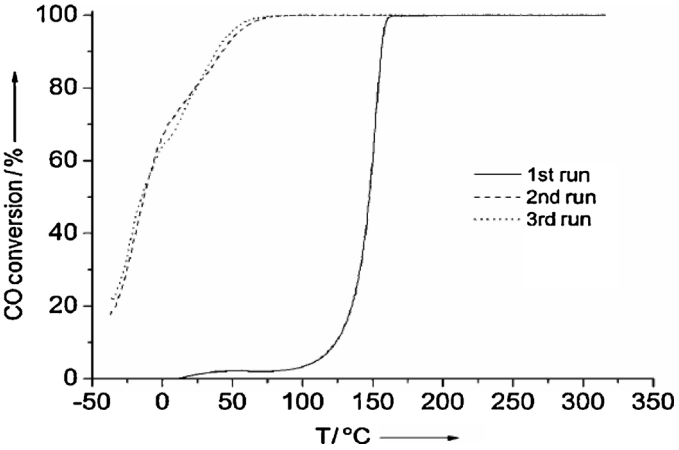

Fig. 2. CO oxidation curves for the 1.22% Au/FeO_x catalyst by the gas mixture (composition, vol%: CO—1, O_2—20, N_2—balance), space velocity 80,000 ml/g_{cat}/h. From Ref. [83].

activity of the catalyst is not high and, accordingly, the amount of heat released by the reaction is small, the hot spot occurs at the reactor outlet. However, as the bed heats up, the increasing temperature causes an increase in the catalytic activity and, eventually, an upstream shift of the hot spot [62].

The location of the hot spot at the bed inlet is typical of reactions occurring in the CSI regime: the reaction rate is so high that a small amount of catalyst is sufficient for practically complete conversion of the so-called critical reactant.

In the reaction considered here, the critical reactant is oxygen, whose initial concentration is insufficient for the complete oxidation of CO and H_2 together. Its steady-state residual concentration is at the 30 ppm level (Fig. 1).

Note that, in the transition of the reaction to the CSI regime, the residual CO concentration passes through a minimum. This is due to the fact that, as the temperature rises, the activity of the catalyst increases, but the selectivity decreases at the same time [37,66].

The slow and slight increase in both temperature (T_{inlet}) and CO concentration observed after the transition of the reaction to the external diffusion control regime might be due, to the reactor walls heating up in the course of establishment of heat balance in the catalyst–reactor–environment system.

While the plot of the reactant conversion versus the hot spot temperature is a smooth monotonic curve, the curve of conversion versus heater temperature has a segment parallel to the ordinate axis, indicating a transition of the reaction to the external diffusion control regime [62].

Accordingly, the abrupt increase in the CO conversion as a result of a small change in the temperature may be due to transition of the reaction to ignition regime. In this, the temperature is measured outside the hot spot of the catalyst bed.

By way of example, we will consider data for CO oxidation in the linear heating regime over a 1.22% Au/FeO_x catalyst in a 1% CO, 20% O_2, N_2 balance mixture [83] (Fig. 2). (The catalyst was prepared by colloidal precipitation from a $HAuCl_4$ solution in the presence of polyvinyl alcohol (PVA). The reducing agent was sodium tetrahydroborate. The conversion of Au(III) into gold metal was revealed as the color of the solution changed to orange-brown.)

As demonstrated in Fig. 2, the CO conversion over the initial catalyst heated to ~125 °C was low (1st run). (It is significant that the measuring thermocouple was placed over the catalyst bed inlet, measuring the temperature of the gas heated by the external heater). At further heating, the CO conversion increased rapidly: as the temperature was raised from 140 to 150 °C, the conversion increased from ~30% to ~80%, and was total at 160 °C. It is this kind of a dependence of catalytic activity on the temperature of the entering gas that is characteristic of CSI [42,62].

In the next heating cycles (2nd and 3rd runs), the CO conversion reached 100% at substantially lower temperatures, indicating the activation of the catalyst in the first run. Since gold in the catalyst sample was originally reduced to gold metal, the low initial catalytic activity might be due to the adhesion of a polyvinyl alcohol film to it (gold). This film impeded the CO oxidation reaction, but it broke down on heating.

The transition of the reaction to the external diffusion control regime must be accompanied by a marked decrease in the activation energy. Thus, a bend in the Arrhenius plots for CO oxidation was observed in [84,85] and also discussed in [8] for a number of Au/TiO_2-catalysts: at an increase in temperature the activation energy decreases by an order of magnitude. This effect is interpreted as a change in the properties of active centers [8]. In our opinion, it is a consequence of the reaction transition into the external diffusion control regime when the temperature is raised.

For some catalysts involved in preferential CO oxidation, the linear plot of the logarithm of H_2 conversion as a function of inverse temperature shows a bend and the activation energy at lower temperatures is approximately twice that of the activation energy at higher temperatures [35]. The O_2 conversion reaches 100% at the bend temperature (the total CO, O_2, and H_2 concentration is 4 vol%), again pointing at the transition of the reaction to external diffusion control regime. This result was interpreted [35] on the basis of specific features of H_2 oxidation in the presence of CO, without taking exothermicity of the reaction into consideration.

It is clear from the above analysis that if the temperature is not monitored simultaneously at least at the inlet and outlet, it will be difficult to correlate the residual CO and O_2 concentrations with the corresponding hot spot temperature. For instance, CO oxidation is rather commonly investigated in the linear heating regime using a single thermocouple either outside or inside the bed to monitor the state of the catalyst [10,32,35,37,39,83,86–89]. The information about temperature dependence of CO conversion and selectivity received from such a set-up is likely to be distorted because of the shift of the hot spot during heating.

Note that the dilution of the catalyst with an inert material, an expedient used to reduce the effect of the exothermicity of the reaction, does not change the heat of the reaction, but affects heat removal by increasing the reaction zone–reactor wall contact area. This somewhat enhances heat transfer through the reactor walls, thus raising the critical ignition temperature.

We assumed the above by default that the heat released during the reaction exerts no effect on the heat flow from the external heater. In the strict sense, this is not true, but the effect of the heat of the reaction on the operation of the heater can be neglected when the control thermocouple of the heater is outside the reaction zone. And what will happen if the control thermocouple is introduced in the catalyst bed? The heat flow to the thermocouple will increase with increase in conversion because of the reaction. In response to this increase in the heat flow, which will be detected by the thermocouple, the heater will reduce its heat input. As a result, there can be a failure of ignition. We think that it is this effect that was encountered in CO oxidation over Au/TiO_2 under linear heating [87]: the CO conversion versus temperature curve showed an abrupt initial jump followed by a descending portion and a monotonically ascending portion (Fig. 3, 2nd–4th runs).

2.2. Temperature and feed flow rate effects in the operation in the external diffusion control regime: Hysteresis

An exothermic reaction switches to external diffusion control regime once the critical ignition temperature (T_i) reaches the hot spot, when the heat generated by the reaction begins to exceed the

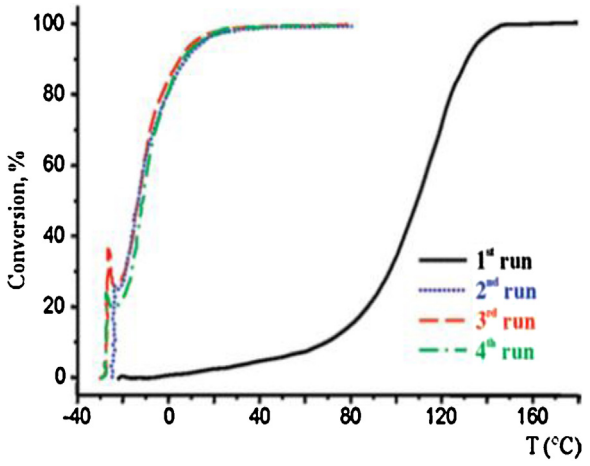

Fig. 3. CO oxidation curves for the 1% Au/TiO_2 catalyst (PVA-protected) by the gas mixture (composition, vol%: CO—1, O_2—20, N_2—balance), space velocity 80,000 $ml/g_{cat}/h$. From Ref. [87].

heat removed with the gas flow and also through reactor walls. The critical temperature can be attained in several ways. As the temperature of the external heater is raised, the activity of the catalyst increases and the heat balance changes in favor of heat buildup. The reaction can also be brought into the CSI regime by increasing the feed flow rate. This leads to an increase in the amount of reactant converted and, accordingly, to an increase in heat generation. Finally, the reaction can be initiated in the external diffusion control regime by supplying the reactants at an above-critical temperature.

After the transition of the reaction to the CSI regime, variation of the heater temperature and feed flow rate in certain ranges does not bring the reaction back from the ignition regime [42,66,70]. This allows the catalyst operation conditions to be optimized. As the temperature is lowered, the hot spot remains at the bed inlet and oxygen is almost entirely converted, so the selectivity in the CSI regime is determined only by the residual CO concentration, which decreases as the hot spot cools down.

A hysteresis can be observed in the external diffusion control regime [42,62]: at the same external heater temperature, the residual concentrations of the reactants (CO, O_2) and the catalyst bed temperature during the heating of the system differ from those observed during cooling.

However, the possibility of the system passing to the CSI regime is sometimes disregarded in the analysis of the causes of this hysteresis. For example, the hysteresis in preferential CO oxidation over a ceria-supported catalyst containing 0.28 at% Au and Ge and Gd dopants is attributed to catalyst activation [32]. The hysteresis in H_2 oxidation over Au/Al_2O_3 is explained by the adverse effect of water during heating [35]. A hysteresis was also observed for the as-prepared 2.6% $Au/Ce_{0.62}Zr_{0.38}O_2$ catalyst under linear temperature variation (heating and cooling) [90]. The activity of this catalyst increased even after heating was stopped. The authors of that study rightly believe that heating activates the catalyst, but it would be more correct to consider catalyst activation in combination with surface ignition.

Both the return of a reaction from the external diffusion control regime and the transition of the reaction to this regime show themselves in the form of a temperature jump: once the critical extinction temperature is reached, the conversion falls abruptly. This phenomenon was observed for Co_3O_4 and Au/Co_3O_4 catalysts under cooling and was interpreted as their deactivation [91].

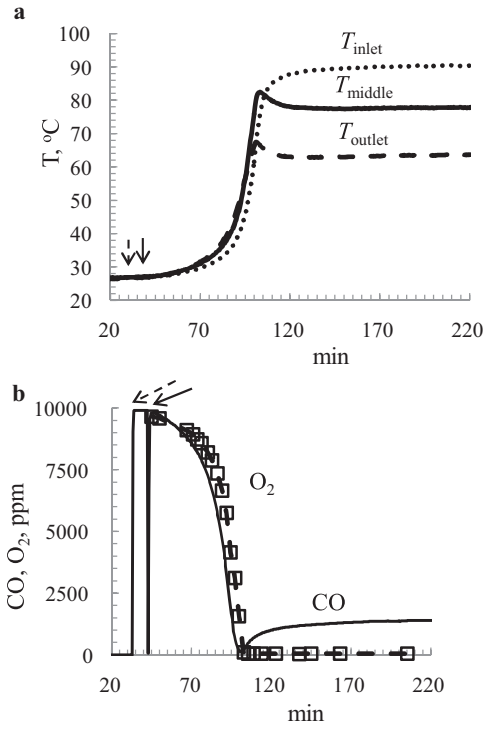

Fig. 4. Activation of the 1% Au/Al_2O_3 catalyst precursor (a bed height of ~1.6 cm) by the gas mixture (composition, vol%: O_2—0.99, CO—0.97, H_2—60, N_2—balance) at room temperature. a—dynamics of the temperature at the bed: inlet—T_{inlet}, outlet—T_{outlet}, and the middle of the bed—T_{middle}; b—dynamics of the residual CO and O_2 content. Dashed and solid lines indicate the gas bypassed the reactor and supplied to the reactor, respectively. GHSV 39 $N\,l/g_{cat}/h$. From Ref. [71].

2.3. Factors hampering the transition of the reaction to the CSI regime

We have considered the specific features of the transition of the reaction to the CSI regime earlier and the steady-state run of the reaction in this regime. Now we will turn to factors opposing the transition of the reaction to the CSI regime.

Gold in the catalyst precursors prepared by the deposition–precipitation (DP) or coprecipitation (CP) method was reported to be entirely or partially in cationic form [14,54,92–95]. When the reaction mixture acts on such a precursor, the reaction takes place in parallel with gold activation and this has an effect on the transition of the reaction to the CSI regime.

Data pertaining to the $1\%Au/Al_2O_3$ catalyst prepared by adsorption impregnation followed by drying at 90 °C [71] are presented in Fig. 4. The reactor was purged with hydrogen and then cut off. The reaction mixture was initially by-passed and then directed to the reactor. Slow self-activation of the catalyst was observed over approximately 1 h, which showed itself as a gradual heating of the bed (Fig. 4a) and, accordingly, as a decrease in the residual CO and O_2 concentrations (Fig. 4b). After the temperatures in the bed middle and at the bed outlet reached their maximum values, a steady-state temperature distribution was established in the bed, with the hot spot located at the bed inlet. Thus, the catalyst was activated and the reaction shifted to external diffusion control regime.

A comparison between Figs. 1 and 4 demonstrates that the low initial activity of the precursor leads to a long self-activation period. As mentioned above, gold in the precursor is mainly in oxidized state. The presence of some amount of gold metal provides the initial catalytic activity. In turn, reactions of CO, H_2 oxidation raise the bed temperature, assisting the gradual self-activation of the

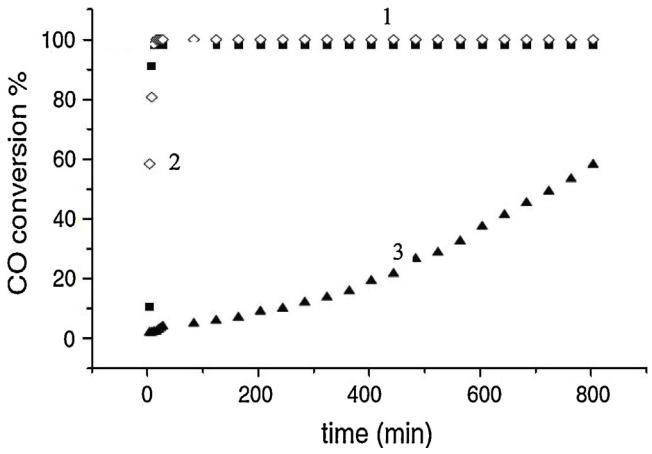

Fig. 5. CO oxidation at 25 °C using dried 2.6%Au/ZnO catalyst precursors by CO/synthetic air (CO_2-free) with a molar ratio of 0.5/99.5. Temperature of precipitation of catalysts: 1–60 °C, 2–80 °C, 3–90 °C. Flow rate 20 ml/min, catalyst loading of 50 mg. From Ref. [12].

catalyst. Activation brings gold into Au^0 state, and this is confirmed by a change in the catalyst color: while the original sample is white, the activated sample is aureate, which is characteristic of gold metal.

Taking these results into account, we will consider data reported for CO oxidation over 2.6% Au/ZnO precursors [12] (Fig. 5). These samples were prepared by coprecipitation followed by drying the washed precipitate at 90 °C. The oxidation of CO was studied at 25 °C (in a quartz reactor immersed in a thermostat) in a flowing CO/artificial air mixture (0.5:99.5 mol/mol). The CO conversion for the samples prepared by precipitation at 60 and 80 °C reaches 100% in a short time (Fig. 5, curves 1 and 2), while the sample precipitated at 90 °C is activated slowly (curve 3). A comparison of Fig. 5 with Figs. 1 and 4 readily demonstrates the following. In the case of samples prepared by precipitation at 60 and 80 °C [12], gold is in highly active state and reaction passes to external diffusion control regime. The sample precipitated at 90 °C, however, shows the same behavior as the 1%Au/Al_2O_3 precursor (Fig. 4).

There has been a report on the transition of CO oxidation to external diffusion control regime at room temperature over an Au/Fe_2O_3 precursor prepared by precipitation followed by drying at 80 °C [47]; however, this transition was not identified by the authors and was considered as interference. In this experiment, as a 5% CO, 20% O_2, Ar balance mixture was fed at a rate of 1000 ml/min into a reactor containing 20 mg of the catalyst, the CO conversion jumped to 100% and the catalyst heated to 120 °C.

The self-activation of a number of Au/Al_2O_3 catalysts in H_2 oxidation and preferential CO oxidation was observed in our earlier study [66], and it can be interpreted as a combination of gold activation and the exothermic reaction.

The transition of the reaction to the CSI regime can be opposed by the strong adsorption of one of the components. For example, strong oxygen adsorption is typical of ruthenium catalysts [67,68]. Accordingly, spontaneous oscillations over a period of several hours can be observed in CO oxidation over these catalysts [68]. The oscillation cycle begins with a slow decrease in the residual CO concentration accompanied by an increase in bed temperature. This process takes place until the critical bed temperature at which rapid ignition occurs. After a short interval, the reaction undergoes equally rapid extinction and the slow activation of the catalyst resumes. We think that these oscillations are due to a combination of strong oxygen adsorption with the exothermicity of the CO oxidation reaction.

The same phenomenon was observed in CO oxidation with a mixture containing a large stoichiometric excess of oxygen on a Pd wire [96], but it was explained by the palladium surface passing into a hyperactive state.

As the hydrogen oxidation and CO oxidation reactions are very exothermic, this exerts a considerable effect on the observed kinetics. Neglect of this circumstance leads to difficulties in data interpretation.

3. Behavior of nanosized gold

3.1. Particle size distribution of gold metal

Gold metal particles in supported catalysts are commonly characterized by electron microscopy. The corresponding histograms demonstrate that the gold particle size distributions for various supports are typically asymmetric, with a maximum shifted to smaller sizes (see, e.g. [28,35,48,83,88,90,92,97,55,98–109]).

This size distribution asymmetry is typical of metal particles in supported metal catalysts, suggesting that the distribution most likely obeys a lognormal law, which is characteristic of a certain class of systems [110]. In these systems the total mass/volume of objects is limited and the increase in the mass of an object during the formation of the system is proportional to the current mass of the object, even though it takes place in a random way. The lognormality of the gold particle size distribution was confirmed for a number of supported Au catalysts by small-angle X-ray scattering and transmission electron microscopy [111]. The reliability of an estimate of the proportion of particles smaller than 1 nm is determined by the class of the electron microscope. Note that a simple test for lognormality of distribution is the linearization of integral distribution in probabilistic logarithmic coordinates [110]. This is illustrated in Fig. 6 where the differential (a and b) and integral (c) gold particle size distributions are given. The latter plot (Fig. 6c) confirms that in both cases (curves 1 and 2) the distribution most likely obeys a lognormal law. Thus, integral particle size distribution eliminates the issue of the arbitrariness in choosing a size interval.

If a gold-containing catalyst is synthesized under fairly mild conditions (at rather low temperatures) on a support with a large specific surface area, then, at a gold content of a few weight percent, the size of the resulting gold particles will be below 10 nm [28,35,48,83,88,90,92,97,55,98–109].

An increase in the gold content must cause accretion of separate particles to increase the proportion of larger particles. For example, there has been a study of Au onto the TiC (0 0 1) surface [107]. Au was vapor-deposited on TiC (0 0 1) at room temperature. At gold coverage of 0.1 and 0.5 ML (ML = monolayer), the resulting gold particle size distribution has a "tail" on the larger particle side. By contrast, at a gold coverage of 1.5 ML, the tail is on the smaller size side of the distribution peak.

As the heat treatment temperature is raised, the distribution profile shifts to larger particle sizes [61,102,103,112,113]. The same effect is observed as the gold content is increased [48].

The effect of catalysis on the particle size distribution of gold is insignificant [88,106,114].

3.2. On the "size effect" in gold catalysts

As noted above, the size of gold particles in supported catalysts varies in a fairly wide range. This brings up the issue of interpreting the size effect for supported Au catalysts [3,89,115–120]. The effect was first observed by Haruta and his colleagues [115] for Au/Co_3O_4, Au/Fe_2O_3, and Au/TiO_2 catalysts and is now actively discussed by researchers. The current situation in this area is precisely

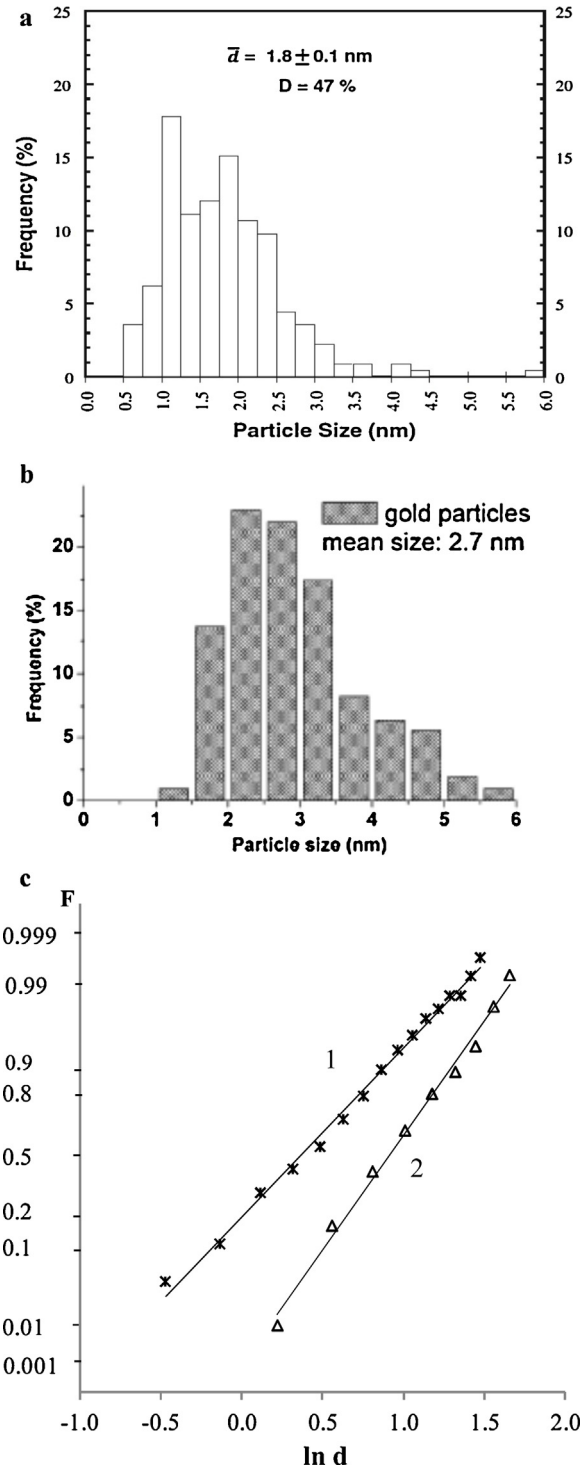

Fig. 6. Differential (a and b) and integral (c) gold particle size distribution for Au/CZ-DPU-OE523 (a) and Au/$MgFe_2O_4$ (b) catalysts. (c)—Linearization of distributions in the probabilistic logarithmic coordinates; 1—Au/CZ-DPU-OE523; 2—Au/$MgFe_2O_4$. Differential distributions from: Ref. [90] (a) and Ref. [88], Supplementary (b).

characterized as follows [121]: "A twist about an atomistic explanation for the unusual particle size-dependent reactivity enhancement of supported gold clusters still exists in the surface science and catalysis communities".

Note that a physically meaningful correlation is the dependence of catalytic activity on particle size, not on the mean value of the size distribution. The possible causes of such dependence have been discussed in earlier works [122,123]. In this case, if there is a particle

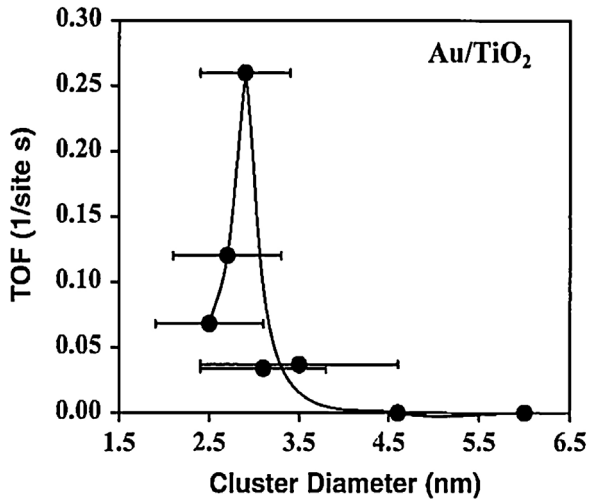

Fig. 7. CO oxidation turnover frequencies (TOF) at 300 K as a function of the average size of the Au particles supported on a high surface area TiO_2 support. From Ref. [117].

size distribution, the activity of the catalyst will reflect the integral activity over this distribution; that is, it will depend on distribution parameters (mean value and dispersion).

However, many studies have dealt with the dependence of catalytic activity on the mean of the particle size distribution [3,89,115–120]. When correlating catalytic activity with cluster size, some authors [116–120] did not take into account that the gold surface area available for catalysis may vary from one sample to another (samples with different gold contents were examined).

As for Haruta's works on Au/TiO_2 catalysts, detailed data suggesting the existence of a size effect are presented in [89] (Table 1). These data were discussed in some way in other works [3,116–118,124,125] and led to the correlation plotted in Fig. 7 [116,117].

By correlating catalytic activity with the mean crystallite size for the samples listed in Table 1, the size effect was observed: an extremely high activity was seen for a mean particle size of ~3 nm [3,115,117]. Indeed, as seen from the data presented in Table 1, the mean particle size varies only slightly, particularly in samples 1–5, but all activity characteristics ($T_{1/2}$, W, TOF) change significantly.

In our opinion, there are no sufficient grounds to claim the existence of a size effect in this case. First, samples 1–5 differ essentially from samples 6 and 7 in their synthesis [89], so it would be correct to compare data for samples 1–5 only. Second, strictly speaking, it is preferable to make a correlation of experimental activity data with the accessible surface area of gold particles estimated by an independent method. But even within the framework of the approaches taken in [89], we can see the following: estimation of TOF from the CO oxidation rate extrapolated to 300 K with estimation of the number of accessible gold atoms from the mean particle size suggests that catalytic activity depends on the gold content only. It can indeed be seen in Fig. 8 that $T_{1/2}$ and TOF correlate well with the gold content. The CO oxidation rate as a function of gold content behaves in the same way as TOF. Moreover, as demonstrated in the insert in Fig. 8, the mean crystallite size also correlates with the gold content of the samples.

An examination of the correlations plotted in Fig. 8 suggests that there is no size effect on catalytic activity in this case, as the dependence of both TOF and particle size on Au content is basically monotonous considering errors in experimental and calculated values. Thus, the extremum in the correlation presented in Fig. 7 is a result of the interplay of the following factors: dependence of the

Table 1
[*]Gold content, mean particle size, and activity data for Au/TiO_2 catalysts [89].

Entry	Catalyst	Au content, (wt%)	Mean particle size (nm)	$T_{1/2}$ (K)	W, 10^{-7} (mol/s/g_{cat})	TOF (s^{-1})
1	0.5%Au-DP	0.5	2.5	320	3.80	3.7×10^{-2}
2	0.7%Au-DP	0.7	2.7	282	6.90	3.4×10^{-2}
3	1.8%Au-DP	1.8	2.9	253	55	1.2×10^{-1}
4	2.3%Au-DP	2.3	3.1	235	45	6.8×10^{-2}
5	3.1%Au-DP	3.1	3.5	235	200	2.6×10^{-1}
6	1.0%Au-FD	1	4.6	477	0.0015	9.6×10^{-6}
7	3.6%Au-FD	3.6	6	443	0.0036	8.3×10^{-6}

[*] DP = synthesis by deposition, FD = "photochemical" synthesis, $T_{1/2}$ = temperature corresponding to 50% conversion of 1% CO in air, and W = CO oxidation rate at 300 K calculated from the Arrhenius dependence of the oxidation rate on inverse temperature. The turnover frequency (TOF) was calculated under the assumption that the number of gold atoms on the surface is determined by the mean particle size and the particles are cubic.

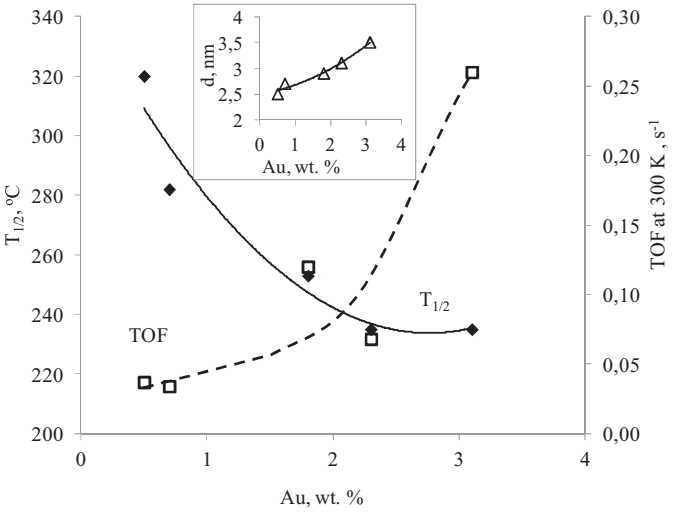

Fig. 8. Correlation of turnover frequencies of CO oxidation (TOF) and temperature of 50% conversion CO ($T_{1/2}$) with Au content of the catalysts. Insert shows the correlation of the average size of Au particles with Au content of the catalysts (according to data [89]).

catalytic activity on gold content, roughness of TOF estimate, choice of samples synthesized by different methods.

The absence of size effect was also inferred from a study of the catalytic activity, at 298 K, of a series of 4.5 wt% Au/TiO_2 samples differing in their mean crystallite size calculated from EXAFS data [124].

4. Conclusions

An extensive body of data on CO oxidation and PROX (preferential CO oxidation) over supported gold catalysts has been discussed. Under certain conditions, the exothermicity of CO oxidation or PROX brings the reaction into external diffusion control regime. This shows itself as a number of experimentally observable effects (jump of conversion as a result of temperature variation, CO conversion hysteresis, appearance of a hot spot, and precursor self-activation). Transition to this regime sharply decreases apparent activation energy.

In a reductive medium or after the heat treatment, gold in the catalyst is typically in the form of metal particles with a lognormal size distribution. Size effect data indicating the existence of an extremum of catalytic activity as a function of mean particle size have been revised.

It has been demonstrated that for samples synthesized under the same conditions [89], catalytic activity varies monotonically with gold content rather than with the mean particle size of gold.

Acknowledgments

Author would like to thank his colleagues E.A. Volnina and I.N. Zavalishin for useful discussions. This work has been done with the support of Russian Foundation for Basic Research (grant no. 09-03-00226).

References

[1] M. Haruta, T. Kobayashi, H. Sano, N. Yamada, Chem. Lett. 16 (1987) 405–408.
[2] M. Haruta, N. Yamada, T. Kobayahsi, S. Minima, J. Catal. 115 (1989) 301–309.
[3] M. Haruta, Gold Bull. 37 (2004) 27–36.
[4] M. Haruta, CATTECH 6 (2002) 102–115.
[5] Y. Zhang, X. Cui, F. Shi, Y. Deng, Chem. Rev. 112 (2012) 2467–2505.
[6] Y. Mikami, A. Dhakshinamoorthy, M. Alvaro, H. García, Catal. Sci. Technol. 3 (2013) 58–69.
[7] G.C. Bond, D.T. Thompson, Catal. Rev. Sci. Eng. 41 (1999) 319–388.
[8] T. Takei, T. Akita, I. Nakamura, T. Fujitani, M. Okumura, K. Okazaki, J. Huang, T. Ishida, M. Haruta, Adv. Catal. 55 (2012) 1–126.
[9] H.H. Kung, M.C. Kung, C.K. Costello, J. Catal. 216 (2003) 425–432.
[10] S. Ivanova, C. Petit, V. Pitchon, Appl. Catal., A 267 (2004) 191–201.
[11] R. Zanella, S. Giorgio, C.-H. Shin, C.R. Henry, C. Louis, J. Catal. 222 (2004) 357–367.
[12] S. Al-Sayari, A.F. Carley, S.H. Taylor, G.J. Hutchings, Top. Catal. 44 (2007) 123–128.
[13] S. Sciré, C. Crisafulli, P.M. Riccobene, G. Patané, A. Pistone, Appl. Catal., A 417–418 (2012) 66–75.
[14] J.H. Yang, J.D. Henao, C. Costello, M.C. Kung, H.H. Kung, J.T. Miller, A.J. Kropf, J.-G. Kim, J.R. Regalbuto, M.T. Bore, H.N. Pham, A.K. Datye, J.D. Laeger, K. Kharas, Appl. Catal., A 291 (2005) 73–84.
[15] A. Wolf, F. Schuth, Appl. Catal., A 226 (2002) 1–13.
[16] S. Ivanova, V. Pitchon, Y. Zimmermann, C. Petit, Appl. Catal., A 298 (2006) 57–64.
[17] S. Ivanova, V. Pitchon, C. Petit, H. Herschbach, A. Van Dorsselaer, E. Leize, Appl. Catal., A 298 (2006) 203–210.
[18] Y. Azizi, V. Pitchon, C. Petit, Appl. Catal., A 385 (2010) 170–177.
[19] F. Moreau, G.C. Bond, A.O. Taylor, J. Catal. 231 (2005) 105–114.
[20] C. Baatz, N. Decker, U. Prüße, J. Catal. 258 (2008) 165–169.
[21] A. Hugon, N.E. Kolli, C. Louis, J. Catal. 274 (2010) 239–250.
[22] M. Daté, M. Okumura, S. Tsubota, M. Haruta, Angew. Chem. Int. Ed. 43 (2004) 2129–2132.
[23] C.K. Costello, O.P. Yang, P.H. Law, Y. Wang, J.-N. Lin, L.D. Marks, M.C. Kung, H.H. Kung, Appl. Catal., A 243 (2003) 15–24.
[24] T.A. Ntho, J.A. Anderson, M.S. Scurell, J. Catal. 261 (2009) 94–100.
[25] R.A. Ojifinni, N.S. Froemming, J. Gong, M. Pan, T.S. Kim, J.M. White, G. Henkelman, C.B. Mullins, J. Am. Chem. Soc. 130 (2008) 6801–6812.
[26] F. Gao, T.E. Wood, D.W. Goodman, Catal. Lett. 134 (2010) 9–12.
[27] B.L. Moroz, P.A. Pyrjaev, V.I. Zaikovskii, V.I. Bukhtiyarov, Catal. Today 144 (2009) 292–305.
[28] P.A. Pyryaev, B.L. Moroz, D.A. Zyuzin, A.V. Nartova, V.I. Bukhtiyarov, Kinet. Catal. 51 (2010) 885–892.
[29] M. Shou, H. Takekawa, D.-Y. Ju, T. Hagiwara, D. Lu, K. Tanaka, Catal. Lett. 108 (2006) 119–124.
[30] J. Gong, C.B. Mullins, Acc. Chem. Res. 42 (2009) 1063–1073.
[31] T.S. Kim, J. Gong, R.A. Ojifinni, J.M. White, C.B. Mullins, J. Am. Chem. Soc. 128 (2006) 6282–6283.
[32] W. Deng, J. De Jesus, H. Saltsburg, M. Flytzani-Stephanopoulos, Appl. Catal., A 291 (2005) 126–135.
[33] G. Avgouropoulos, T. Ioannides, Ch. Papadopoulou, J. Batista, S. Hocevar, H.K. Matralis, Catal. Today 75 (2002) 157–167.
[34] C.K. Costello, M.C. Kung, H.-S. Oh, Y. Wang, H.H. Kung, Appl. Catal., A 232 (2002) 159–168.
[35] R.J.H. Grisel, B.E. Nieuwenhuys, J. Catal. 199 (2001) 48–59.
[36] M. Ojeda, B.-Z. Zhan, E. Iglesia, J. Catal. 285 (2012) 92–102.
[37] E. Quinet, L. Piccolo, F. Morfin, P. Avenier, F. Diehl, V. Caps, J.-L. Rousset, J. Catal. 268 (2009) 384–389.

[38] E. Quinet, F. Morfin, F. Diehl, P. Avenier, V. Caps, J.-L. Rousset, Appl. Catal., B 80 (2008) 195–201.
[39] E. Quinet, L. Piccolo, H. Daly, F.C. Meunier, F. Morfin, A. Valcarcel, P. Avenier, V. Caps, J.-L. Rousset, Catal. Today 138 (2008) 43–49.
[40] M. Azar, V. Caps, F. Morfin, J.-L. Rousset, A. Piednoir, J.-C. Bertolini, L. Piccolo, J. Catal. 239 (2006) 307–312.
[41] H. Imai, M. Daté, S. Tsubota, Catal. Lett. 124 (2008) 68–73.
[42] M. Kipnis, E. Volnina, Appl. Catal., B 98 (2010) 193–203.
[43] L. Piccolo, H. Daly, A. Valcarcel, F.C. Meunier, Appl. Catal., B 86 (2009) 190–195.
[44] M.C. Kung, R.J. Davis, H.H. Kung, J. Phys. Chem. C 111 (2007) 11767–11775.
[45] S. Peters, S. Peredkov, M. Neeb, W. Eberhardt, M. Al-Hada, Surf. Sci. 608 (2013) 129–134.
[46] P. Jiang, S. Porsgaard, F. Borondics, M. Köber, A. Caballero, H. Bluhm, F. Besenbacher, M. Salmeron, J. Am. Chem. Soc. 132 (2010) 2858–2859.
[47] M. Khoudiakov, M.C. Gupta, S. Deevi, Appl. Catal., A 291 (2005) 151–161.
[48] M. Méndez-Cruz, J. RamÍrez-SolÍs, R. Zanella, Catal. Today 166 (2011) 172–179.
[49] A.V. Simakov, V.V. Kriventsov, I.L. Simakova, E.V. Smolentseva, F. Castillon, M. Estrada, E. Vargas, E.P. Yakimchuk, D.P. Ivanov, D.G. Aksenov, D.V. Andreev, B.N. Novgorodov, D.I. Kochubey, S. Fuentes, J. Surf. Invest. 4 (2010) 630–635.
[50] N.F.P. Ribeiro, R.P.F. Bonfim, M.M.V.M. Souza, M. Schmal, J. Power Sources 195 (2010) 7386–7390.
[51] J.C. Fierro-Gonzalez, B.C. Gates, J. Phys. Chem. B 108 (2004) 16999–17002.
[52] J. Guzman, B.C. Gates, J. Am. Chem. Soc. 126 (2004) 2672–2673.
[53] J.C. Fierro-Gonzalez, J. Guzman, B.C. Gates, Top. Catal. 44 (2007) 103–114.
[54] C.K. Costello, J. Guzman, J.H. Yang, Y.M. Wang, M.C. Kung, B.C. Gates, H.H. Kung, J. Phys. Chem. B 108 (2004) 12529–12536.
[55] X. Liao, W. Chu, X. Dai, V. Pitchon, Appl. Catal., A 449 (2012) 131–138.
[56] Q. Fu, H. Saltsburg, M. Flytzani-Stephanopoulos, Science 301 (2003) 935–938.
[57] S. Carrettin, A. Corma, M. Iglesias, F. Sánchez, Appl. Catal., A 291 (2005) 247–252.
[58] J. Guzman, S. Carrettin, A. Corma, J. Am. Chem. Soc. 127 (2005) 3286–3287.
[59] P. Concepción, S. Carrettin, A. Corma, Appl. Catal., A 307 (2006) 42–45.
[60] Y. Liu, B. Liu, Q. Wang, C. Li, W. Hu, Y. Liu, P. Jing, W. Zhao, J. Zhang, J. Catal. 296 (2012) 65–76.
[61] M.P. Casaletto, A. Longo, A.M. Venezia, A. Martorana, A. Prestianni, Appl. Catal., A 302 (2006) 309–316.
[62] A.Ya. Rozovskii, M.A. Kipnis, E.A. Volnina, G.I. Lin, P.V. Samokhin, Kinet. Catal. 48 (2007) 701–710.
[63] M.S. Chen, Y. Cai, Z. Yan, K.K. Gath, S. Axnanda, D.W. Goodman, Surf. Sci. 601 (2007) 5326–5331.
[64] P.-A. Carlsson, M. Skoglundh, Appl. Catal., B 101 (2011) 669–675.
[65] A. Abedi, R. Hayes, M. Votsmeier, W.S. Epling, Catal. Lett. 142 (2012) 930–935.
[66] M. Kipnis, E. Volnina, Appl. Catal., B 103 (2011) 39–47.
[67] A.Ya. Rozovskii, M.A. Kipnis, E.A. Volnina, P.V. Samokhin, G.I. Lin, Kinet. Catal. 49 (2008) 92–102.
[68] A.Ya. Rozovskii, M.A. Kipnis, E.A. Volnina, P.V. Samokhin, G.I. Lin, M.A. Kukina, Kinet. Catal. 50 (2009) 691–704.
[69] A.Ya. Rozovskii, G.I. Lin, M.A. Kipnis, P.V. Samokhin, E.A. Volnina, I.A. Belostotsky, G.M. Grafova, I.N. Zavalishin, Top. Catal. 42–43 (2007) 437–441.
[70] M.A. Kipnis, E.A. Volnina, Kinet. Catal. 51 (2010) 279–287.
[71] M.A. Kipnis, E.A. Volnina, A.A. Ezhov, V.K. Ivanov, Kinet. Catal. 54 (2013) 358–368.
[72] D.A. Frank-Kamenetskii, Diffusion and Heat Transfer in Chemical Kinetics, Plenum Press, New York, NY, 1969.
[73] C.N. Satterfield, Heterogeneous Catalysis in Industrial Practice, Krieger Publishing Company, Malabar, FL, 1996.
[74] D.H. Han, O.O. Park, Y.G. Kim, Appl. Catal., A 86 (1992) 71–82.
[75] A.N.R. Bos, E. Hof, W. Kuper, K.R. Westerterp, Chem. Eng. Sci. 48 (1993) 1959–1969.
[76] V.A. Kirillov, I.V. Koptyug, Ind. Eng. Chem. Res. 44 (2005) 9727–9738.
[77] A. Jaree, R.R. Hudgins, H.M. Budman, P.L. Silveston, V.Z. Yakhnin, M. Menzinger, Ind. Eng. Chem. Res. 42 (2003) 1662–1673.
[78] P.-A. Carlsson, M. Skoglundh, P. Thormählen, B. Andersson, Top. Catal. 30/31 (2004) 375–381.
[79] A. Beretta, G. Groppi, M. Lualdi, I. Tavazzi, P. Forzatti, Ind. Eng. Chem. Res. 48 (2009) 3825–3836.
[80] D. Oancea, V. Munteanu, D. Razus, M. Mitu, J. Therm. Anal. Calorim. 103 (2011) 911–916.
[81] I. Uriz, G. Arzamendi, P.M. Diéguez, O.H. Laguna, M.A. Centeno, J.A. Odriozola, L.M. Gandía, Catal. Today 216 (2013) 283–291.
[82] G. Arzamendi, I. Uriz, P.M. Diéguez, O.H. Laguna, W.Y. Hernández, A. Álvarez, M.A. Centeno, J.A. Odriozola, M. Montes, L.M. Gandía, Chem. Eng. J. 167 (2011) 588–596.
[83] Y. Liu, C.-J. Jia, J. Yamasaki, O. Terasaki, F. Schüth, Angew. Chem. Int. Ed. 49 (2010) 5771–5775.
[84] M. Haruta, Chem. Rec. 3 (2003) 75–87.
[85] T. Fujitani, I. Nakamura, Angew. Chem. Int. Ed. 50 (2011) 10144–10147.
[86] E.-Y. Ko, E.D. Park, K.W. Seo, H.C. Lee, D. Lee, S. Kim, Catal. Today 116 (2006) 377–383.
[87] M. Comotti, W.-C. Li, B. Spliethoff, F. Schüth, J. Am. Chem. Soc. 128 (2006) 917–924.
[88] C.-J. Jia, Y. Liu, M. Schwickardi, C. Weidenthaler, B. Spliethoff, W. Schmidt, F. Schüth, Appl. Catal., A 386 (2010) 94–100.
[89] G.R. Bamwenda, S. Tsubota, T. Nakamura, M. Haruta, Catal. Lett. 44 (1997) 83–87.
[90] E. del Río, G. Blanco, S. Collins, M.L. Haro, X. Chen, J.J. Delgado, J.J. Calvino, S. Bernal, Top. Catal. 54 (2011) 931–940.
[91] D.A.H. Cunningham, T. Kobayashi, N. Kamijo, M. Haruta, Catal. Lett. 25 (1994) 257–264.
[92] K. Qian, L. Luo, H. Bao, Q. Hua, Z. Jiang, W. Huang, Catal. Sci. Technol. 3 (2013) 679–687.
[93] E.D. Park, J.S. Lee, J. Catal. 186 (1999) 1–11.
[94] J. Xu, P. Li, X. Song, Z. Qi, J. Yu, W. Yuan, Yi-F. Han, Ind. Eng. Chem. Res. 49 (2010) 4149–4155.
[95] Y. Liu, B. Liu, Q. Wang, C. Li, W. Hua, Y. Liu, P. Jing, W. Zhao, J. Zhang, J. Catal. 296 (2012) 65–76.
[96] M.S. Chen, Y. Cai, Z. Yan, K.K. Gath, S. Axnanda, D.W. Goodman, Surf. Science 601 (2007) 5326–5331.
[97] Q. Li, Y. Zhang, G. Chen, J. Fan, H. Lan, Y. Yang, J. Catal. 273 (2010) 167–176.
[98] T. Tabakova, G. Avgouropoulos, J. Papavasiliou, M. Manzoli, F. Boccuzzi, K. Tenchev, F. Vindigni, T. Ioannides, Appl. Catal., B 101 (2011) 256–265.
[99] T. Tabakova, M. Manzoli, D. Paneva, F. Boccuzzi, V. Idakiev, I. Mitov, Appl. Catal., B 101 (2011) 266–274.
[100] L. Ilieva, G. Pantaleo, I. Ivanov, A. Maximova, R. Zanella, Z. Kaszkur, A.M. Venezia, D. Andreeva, Catal. Today 158 (2010) 44–55.
[101] Tana, Fagen Wang, Huaju Li, Wenjie Shen, Catal. Today 175 (2011) 541–545.
[102] L. Ilieva, G. Pantaleo, I. Ivanov, R. Zanella, J.W. Sobczak, W. Lisowski, A.M. Venezia, D. Andreeva, Catal. Today 175 (2011) 411–419.
[103] Na Ta, Jingyue (Jimmy) Liu, Santhosh Chenna, Peter A. Crozier, Yong Li, Aling Chen, Wenjie Shen, J. Am. Chem. Soc. 134 (2012) 20585–20588.
[104] K. Zhao, B. Qiao, J. Wang, Y. Zhang, T. Zhang, Chem. Commun. 47 (2011) 1779–1781.
[105] P. Sangeetha, B. Zhao, Y.-W. Chen, Ind. Eng. Chem. Res. 49 (2010) 2096–2102.
[106] J. Huang, L.-C. Wang, Y.-M. Liu, Y. Cao, H.-Y. He, K.-N. Fan, Appl. Catal., B 101 (2011) 560–569.
[107] J.A. Rodriguez, P. Liu, Y. Takahashi, F. Viñes, L. Feria, E. Florez, K. Nakamura, F. Illas, Catal. Today 166 (2011) 2–9.
[108] U. Hartfelder, C. Kartusch, M. Makosch, M. Rovezzi, J. Sá, J.A. van Bokhoven, Catal. Sci. Technol. 3 (2013) 454–461.
[109] F. Somodi, I. Borbáth, M. Hegedűs, K. Lázár, I.E. Sajó, O. Geszti, S. Rojas, J.L.G. Fierro, J.L. Margitfalvi, Appl. Surf. Sci. 256 (2009) 726–736.
[110] R.R. Irani, C.F. Callis, Particle Size: Measurement, Interpretation, and Application, Wiley, New York, NY, 1963.
[111] G. Cocco, S. Enzo, G. Fagherazzi, L. Schifflni, J. Phys. Chem. 83 (1979) 2527–2538.
[112] H.-S. Oh, J.H. Yang, C.K. Costello, Y.M. Wang, S.R. Bare, H.H. Kung, M.C. Kung, J. Catal. 210 (2002) 375–386.
[113] G.M. Veith, A.R. Lupini, S. Rashkeev, S.J. Pennycook, D.R. Mullins, V. Schwartz, C.A. Bridges, N.J. Dudney, J. Catal. 262 (2009) 92–101.
[114] J.A. Hernandez, S. Gómez, B. Pawelec, T.A. Zepeda, Appl. Catal., B 89 (2009) 128–136.
[115] M. Haruta, S. Tsubota, T. Kobayashi, H. Kageyama, M.J. Genet, B. Delmon, J. Catal. 144 (1993) 175–192.
[116] M. Valden, X. Lai, D.W. Goodman, Science 281 (1998) 1647–1650.
[117] M.S. Chen, D.W. Goodman, Catal. Today 111 (2006) 22–33.
[118] M. Chen, D.W. Goodman, Acc. Chem. Res. 39 (2006) 739–746.
[119] I. Laoufi, M.-C. Saint-Lager, R. Lazzari, J. Jupille, O. Robach, S. Garaudée, G. Cabailh, P. Dolle, H. Cruguel, A. Bailly, J. Phys. Chem. C 115 (2011) 4673–4679.
[120] M.-C. Saint-Lager, I. Laoufi, A. Bailly, O. Robach, S. Garaudée, P. Dolle, Faraday Discuss. 152 (2011) 253–265.
[121] J. Shan, M. Komarneni, U. Burghaus, Chem. Phys. Lett. 517 (2011) 59–61.
[122] B. Hvolbæk, T.V.W. Janssens, B.S. Clausen, H. Falsig, C.H. Christensen, J.K. Nørskov, Nano Today 2 (2007) 14–18.
[123] S.H. Brodersen, U. Grшnbjerg, B. Hvolbæk, J. Schiøtz, J. Catal. 284 (2011) 34–41.
[124] S.H. Overbury, V. Schwartz, D.R. Mullins, W.F. Yan, S. Dai, J. Catal. 241 (2006) 56–65.
[125] G.C. Bond, Molecules 17 (2012) 1716–1743.